EARLY EVOLUTION OF A CME FROM WHITE LIGHT AND UV OBSERVATIONS

A. Bemporad[1], G. Poletto[2], and J.C. Raymond[3]

[1] $Astronomy\&SpaceScienceDept., Universityof Firenze, Firenze, Italy, Email: bemporad@arcetri.astro.it$

[2] $INAF - ArcetriAstrophysicalObservatory, Firenze, Italy, Email: poletto@arcetri.astro.it$

[4] $Harvard - SmithsonianCenterforAstrophysics, Cambridge, MA, Email: jraymond@cfa.harvard.edu$

ABSTRACT

At least one third of Coronal Mass Ejections (CMEs) have, in the interplanetary medium, a magnetic flux rope structure, usually referred to as "magnetic cloud". The solar origin of the topology of *in situ* flux ropes is debated: according to recent studies only models invoking magnetic reconnection between Active Regions (ARs) and the large scale overlying structures can adequately account for the characteristics of the CME and magnetic cloud fields. In this work we study the early evolution of a coronal mass ejection (CME) which occurred on January 31, 2000, with the aim of inferring the structure of the CME in the early stage of its development and, possibly, to check whether there is any evidence for an interaction between ARs and background structures. Mauna Loa white light and UVCS UV data allowed us to reconstruct the CME configuration: a comparison of the observed structure with that predicted by the Lin & Forbes (2000) CME model shows the two to be quite similar. Densities of the expanding CME bubble and CME core are also given, together with a tentative estimate of the dimension of the CME bubble. Evidence of interaction between the AR where the CME originates and the background structures is also discussed.

Key words: CME; WL observations; UV Spectroscopy.

1. INTRODUCTION

Most CMEs, independent of whether they are or are not associated with prominence eruptions, originate in Active Regions (Subramanian & Dere, 2001) and, at interplanetary distances, show a helical magnetic structure, usually referred to as "magnetic cloud". The interaction between ARs and the background field has been recently studied by several authors (see, e.g., Luhmann et al., 2003; Leamon et al., 2004) who focussed on the relationship between the local AR field and the large scale ambient fields to get a better understanding of the origin of the helical flux ropes observed in the interplanetary medium. It turns out that an interaction between the ARs and the overlying large scale fields is crucial to the interpretation of the CME and interplanetary phenomena.

In this work we analyze the early stages of a CME that occurred in the NE quadrant on January 31, 2000, for which we have the pre-event data as well as data which cover the first hours of the CME evolution. Our analysis is based on Mauna Loa, LASCO and UVCS observations: unfortunately interplanetary data are not available. However, we are able to identify the CME source region and to provide evidence for the interaction between the AR where the CME originates and the large scale ambient field, which gets disrupted by the CME. Also, the configuration of the CME is compared with that predicted by Lin & Forbes (2000) CME model which holds through the early stages of the CME development.

The paper is organized as follows: in the next Section, we describe the coronal scenario within which the CME occurred and in Section 3, after a brief description of Lin & Forbes (2000) CME model, we compare Mauna Loa and UVCS measurements at a fixed altitude, at different times during the CME evolution, with the CME evolution predicted by the Lin & Forbes model. Densities in the CME core and bubble have been derived and turn out to yield a CME mass consistent with typical values found in the literature. Section 4 concludes the paper: we show how, in the later stages of the CME development LASCO data may provide some evidence for the interaction between the CME and the background field.

2. THE CME SCENARIO

On January 31, 2000, LASCO C2 and C3 coronagraphs observed a CME in the NE quadrant at an approximate latitude of 62°, which propagated in the outer corona at a speed of $\approx 500\ km/s$. Extrapolating backwards in time, with a constant speed, the CME turned out to be ejected at a time $t \leq$ 18:43 UT. Fig. 1 (top left panel) shows the pre-

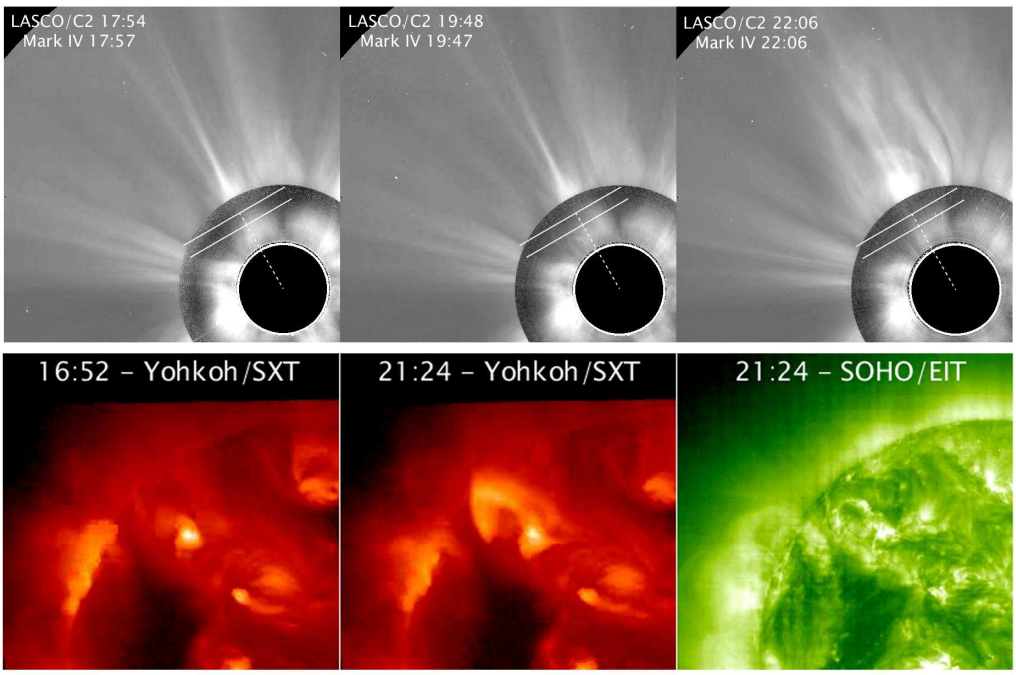

Figure 1. Top: Mauna Loa Mark IV and LASCO C2 images for the CME event on January 31, 2000. Bottom: Yohkoh and EIT images of the activity before and after the CME.

CME corona, from a composite image made up with data taken by the Mauna Loa Mark IV Coronameter and by the LASCO C2 experiment. The middle and right panel give the coronal configuration during the CME propagation. Mark IV pB images are not available after about 22:00 UT. For future reference, the position of the slit of the UVCS spectrometer, set normal to the solar radius at 1.6 and 1.9 solar radii, at a latitude of 60°, is also given in the figure.

In order to identify the source region of the CME we analyzed MDI observations of the ARs on the disk. The most prominent AR in the NE quadrant on January 31 is AR 8851 (at a northern latitude of 27° and eastern longitude of 42°), which is rapidly evolving, with a total area and total sunspot number increasing in time. This rapid evolution implies flux emergence and a possibly unstable configuration that makes AR 8851 a likely candidate for the CME ejection. This identification is further supported by EIT and Yohkoh data: Yohkoh SXT data have a gap in between 16:52 and 21:24 UT, hence there is no data coverage at the time of the CME ejection. However, in the first image available after the gap, at 21:24 UT, a prominent cusp-shaped arch is rooted in AR 8851, and an EIT 195Å loop appears to be nested within the SXT loop (see bottom row in Fig. 1). These newly formed structures provide strong evidence of 8851 being the source of the CME ejection and the site for reconnection of AR fieldlines, torn open by the ejection, and subsequently reforming.

The only alternative source for the CME could be AR 8858, a region which, on January 31, is behind the solar limb and, dragged by solar rotation, crosses the plane of the sky on February 3, at a latitude of 26°. However, disk activity in AR 8851 makes us favor this as the source of the CME. We point out that the low latitude of 8851 (30° southwards of the CME direction of propagation) may not be a problem if plasma is ejected from the cusp of the SXT arch, which seems to project towards higher latitudes.

We may now look for evidence of the magnetic structure that accompanied the CME low in the corona as it first started developing. To this end we briefly recall the basic features of the Lin & Forbes CME model (2000).

3. EVOLUTION OF THE CME STRUCTURE: PREDICTIONS VS. OBSERVATIONS

Over the last few years, Lin & Forbes (2000), Lin, Raymond & Van Ballegooijen (2004), Lin (2004) have thoroughly explored CME processes, from the CME initiation to its expansion through the solar corona and its manifestation at chromospheric levels. During the CME, the field is stretched outwards, due to the catastrophic loss of equilibrium of the flux rope: a current sheet forms in between the reconnecting loops and the lower tip of the bubble that grows around the flux rope as reconnection progresses outward. The temporal evolution of the bubble is illustrated in the top rows of Fig. 2, in a sequence of representative snapshots (from Lin, Raymond & Van Ballegooijen, 2004) that show the magnetic configuration and the bubble expansion at different times. Each panel covers an area of $\approx 2.25 \times 10^{12} Km^2$: starting from the top left panel simulations show the progressive rise of

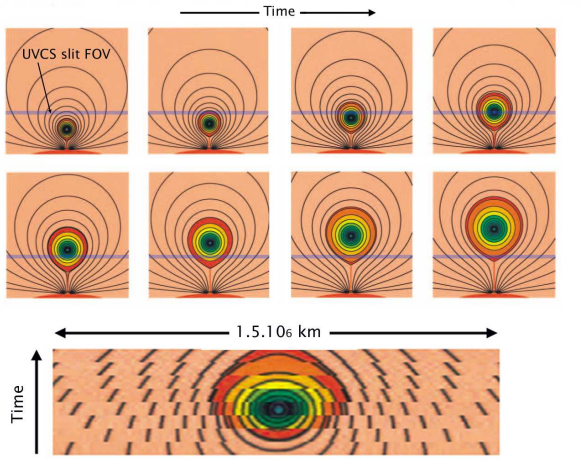

Figure 2. Top: a sequence of snapshots of the CME evolution showing at different times the disrupted magnetic field (from Lin, Raymond & Van Ballegooijen, 2004). Bottom: simulation of the temporal evolution of the CME topology seen through a slit at a fixed altitude, as predicted by the snapshots shown above.

the CME core and the increasing dimensions of the CME bubble. At any given time, because plasma is frozen-in, a thin layer around the separatrix is filled with hot plasma flowing out of the current sheet. Also, plasma in the outer shell is hotter than plasma in the innermost sections.

As we mentioned, UVCS acquired data at 1.6 and 1.9 solar radii: on the snapshots given in Fig. 2 we have drawn a bar, to represent the UVCS slit (width not in scale) and help the reader visualize what UVCS may be expected to observe, if a CME structure happens to be sampled at a fixed altitude during its evolution. Results from a simulation made cutting through the panels of Fig. 2 and letting the rising CME bubble progressively enter a slit set at a constant altitude are shown in the bottom panel of Fig. 2. This represents the temporal evolution of the topology predicted by the Lin & Forbes (2000) model, as seen by a spectrograph slit.

In order to facilitate the comparison between data taken by different experiments, we give in Fig. 3 (left panel) the pB brightness measured at 1.6 solar radii by the Mark IV experiment over a rectangular area that simulates the UVCS slit and, in the right panel, the Lyman-α intensity measured by UVCS at that level, at different times. The similarity between the two data set is not surprising: pB depends on the electron density and, for a fixed outward velocity and approximately constant electron temperature, the Lyman-α intensity is dictated by the electron density as well. In order to enhance the visibility of faint structures, the pB values given in Fig. 3 have been obtained by subtracting from all images the average pB measured, at each latitude, over the whole dataset; the same procedure has been used for the Lyman-α intensity. Notice that Lyman-α observations cover a longer time interval than Mark IV data. Both pB and UVCS data show, until $\approx$ 18:30 UT, a bright emission (between a northern latitude of ≈ 45 and $65°$) which originates from the streamer structure visible in the pre-CME composite Mark IV and LASCO image of Fig. 1, which disappears after the event. At later times, pB and Lyman-α data reveal higher emission at spatially limited locations along the slit. Fig. 3 shows that emission appears at positions along the slit which delineate branches, closely resembling the topology predicted by the Lin & Forbes (2000) model. We conclude that Mark IV and UVCS are sequentially imaging the expanding CME bubble. The bright emitting knot imaged around 20:00 UT at a latitude of $\approx 50°$ may represent the CME core, no longer visible at later times because already moved to higher levels.

We may now evaluate the electron density in the bright features of Fig. 3. To this end we synthesized pre-CME pB values by assuming a priori a reference spherically symmetric density profile (in this case the Guhathakurta et al. 1996 profile) and increasing densities with a constant multiplier until the observed pre-CME pB was reproduced. Once the pre-CME densities have been evaluated, we analogously simulated the CME bright features by increasing densities until observed and reconstructed pB were equal.

In order to infer densities in the bright knot-CME core we assumed either a), a cylindrical structure extending over a depth of one solar radii along the Line of Sight (LOS) and crossing the plane of the sky, or b) a high density spherical blob of plasma along the LOS, at different distances from the plane of the sky. The radius of the spherical blob was assumed to be on the order of 0.1 $R_\odot$, from the size of the knot in pB and Lyman-α images. The density required to reproduce the knot pB turns out to be on the order of $1.8 \cdot 10^7\ cm^{-3}$ and $4.9 \cdot 10^7\ cm^{-3}$, depending on the geometry (a, b, above). With these densities and an estimate of the core volume we calculated respectively a mass on the order of $3.2 \cdot 10^{14}\ g$ and $1.2 \cdot 10^{14}\ g$.

Analogous calculations can be done to evaluate the density in the CME bubble. Density in the outer branch showing up in Fig. 3 is on the order of $1.3 \cdot 10^7\ cm^{-3}$. As a typical dimension of the CME bubble, we may assume a bubble diameter on the order of $1.2 \cdot 10^6\ km$, from the width of area included within the outer branch shown in Fig. 3, which agrees with the bubble size in the simulations of Lin, Raymond & Van Ballegooijen (2004). Should the whole bubble filled with plasma at that density, an order of magnitude estimate of its mass yields a value of about $2.0 \cdot 10^{16}\ g$, which is appropriate for a typical CME. This result implies that the total mass of the CME resides mostly in the CME bubble, while the mass of the CME core is $\sim$ 1/100 of the total CME mass.

4. DISCUSSION AND CONCLUSIONS

In this preliminary analysis of pB, WL and UV observations of a CME that occurred on January 31, 2000, we focussed on the magnetic configuration of the event over the first few hours in its development. We aimed at point-

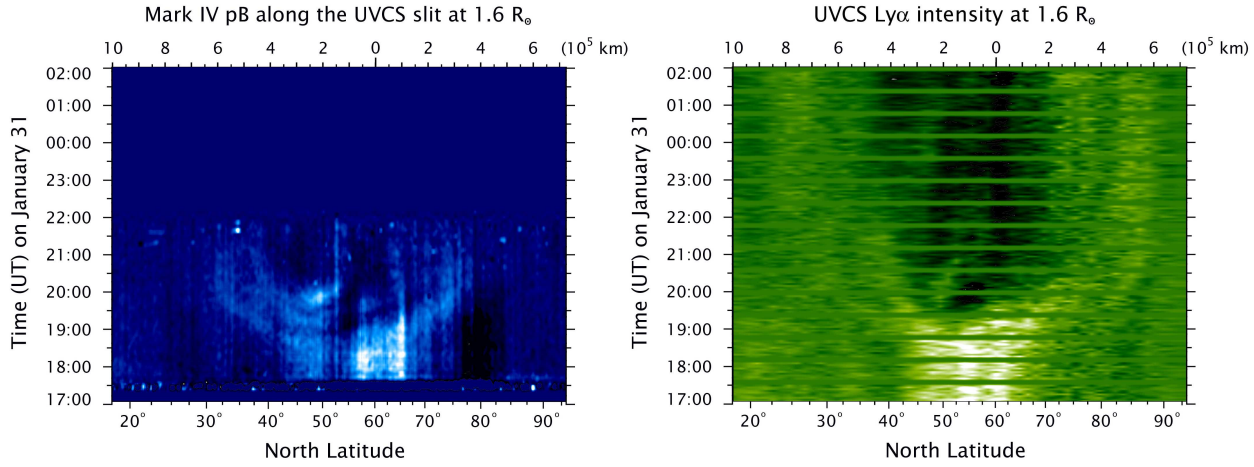

Figure 3. Left: Mark IV pB observed at different times along a slice simulating the UVCS slit, at 1.6 solar radii. Right: Lyman-α intensity at different times, from observations at 1.6 solar radii; the horizontal bars represent time intervals over which data at 1.6 solar radii are missing, because UVCS was observing at 1.9 solar radii.

ing out that the expanding bubble - core CME model of Lin & Forbes (2000) can be identified since the very early stages of the CME and have shown that the CME configuration can be reconstructed in its entirety, even if the event is seen only through a spectrograph slit set at a fixed altitude in the corona. Lyman-α and pB data have been analyzed to infer densities in different sections of the CME and shown to yield a CME mass consistent with typical values found in the literature. Brevity didn't allow us to extend our analysis to the behavior of the OVI emission: here it may suffice to anticipate that because of the higher sensitivity of OVI lines to the temperature variations and Doppler dimming effects, the magnetic configuration is fuzzier in the radiation of OVI lines than it is in Lyman-α radiation (and in pB data). A thorough analysis of available data for this event is in progress.

A last issue which we like to consider is the evidence, or lack of evidence, for interaction between the AR and the background fields. To this end it is worth noticing that, at the time the first SXT loop image is available, the CME had already propagated through the corona and has destroyed the LASCO streamers visible in the pre-CME image at 17:57 UT. This means that the CME originating in 8851 had an impact not only on the AR configuration but also triggered a larger scale disruption and made its way through the open fields that have been created. A "local" field disruption, limited to AR 8851, would not have had an impact on limb structures about 45 degrees distant from the AR. The latter seem to act as channels for the propagation of the CME core while the branch opening (evolving CME bubble) of the streamer background structures (see Fig. 1, top row, right panel) appears like the continuation, at higher altitudes, of the phenomena which have been observed by Mark IV and UVCS in the low corona. Although this is only a qualitative anlysis it seems to confirm the recent findings that AR - background interaction is necessary for the flux rope CME evolution.

ACKNOWLEDGMENTS

This work initiated during a visit of A.B. to the Harvard-Smithsonian Center for Astrophysics whose hospitality and support is gratefully acknowledged. A.B. and G.P. work has been partially supported by COFIN 2003029124_003. SOHO is a mission of international cooperation between ESA and NASA.

REFERENCES

Guhathakurta, M., Holzer, T. E., & MacQueen, R. M., 1996, ApJ, 458, 817

Leamon, R. J., Canfield, R. C., Jones, S. L., Lambkin, K., Lundberg, B. J., & Pevtsov, A., 2004, J. Geophys. Res. 109, A05106, doi:10.1029/2003JA010324

Lin, J., & Forbes, T. G., 2000, JGR 105, 2375

Lin, J., 2004, SP 222, 1375

Lin, J., Raymond, J.C., & Van Ballegooijen, A. A., 2004, ApJ 602, 422

Luhmann, J. G., Li, Y., Zhao, X., Yashiro, S., 2003, SP 213, 367

Subramanian, P. & Dere, K. P., 2001, ApJ 561, 372